.International Journal of Future Generation Communication and Networking
Vol. 13, No. 3, (2020), pp. 2979–2979

Detection and Analysis of Parkinson's Disease Using Piezo Resistive Tactile Mems Sensor

[1],D Sateesh Kumar , [2]P Pardhasaradhi [3]G.R.K.Prasad, [4]N. Ch. Ramgopal

[1]*Associate Professor, Mathematics, Koneru Lakshmaiah Education Foundation, AP, India*
[2]*Professor, ALRC-R&D, ECE, Koneru Lakshmaiah Education Foundation, AP, India*
[3]*Associate Professor, ECE, Koneru Lakshmaiah Education Foundation, AP, India*
[4]*Associate Professor, Mathematics, College of Natural and Computational Science, Bule Hora University, Bule Hora, Ethiopia*
*Corresponding Author Email: drsateeshdeevi@gmail.com

ABSTRACT

In this paper, an accurate methodology is proposed to detect compliance of soft tissue using two serpentine springs as a combined structure in micro machined piezo resistive tactile sensor, small vibrations and variations with live tissue also detected. The measuring range of the sensor is chosen to be associated with the soft-tissue properties. Here 10-80 milli-newton force is applied on the soft tissue and the variations in the tissue are observed, and compared with the existing methods. From the observations, it is found that the sensor output stress sensitivity varies linearly with the variation in applied force. The sensor parameters are optimized to give high sensitivity and linearity of the sensor output. To detect the healthy tissue more force needed to be applied on the proof-mass, which varies the stress applied on the tissue. A light stress is to be applied if it is damaged. Using COMSOL TOOL the design is simulated for checking the sensor performance and compared which micro machined tactile sensor design which is simulated using the ANSYS tool.

Keywords: *Soft tissue, sensitivity, stress, piezo resistive tactile sensor, COMSOL, ANSYS.*

INTRODUCTION

In the 1980s, the movement of innovation gave specialists the capacity to perform surgeries utilizing little therapeutic gear without being in coordinate contact with patients. Such surgeries were called insignificantly intrusive surgeries (MIS) [1]. MIS has a considerable measure of noteworthy benefits contrasted with ordinary open surgeries for specialists and patients. Due to these preferences, MIS are spreading quickly and are relied upon to keep on expanding later on.

In spite of the points of interest related with MIS, they have a few deficiencies that should be overcome. One of the real imperfections is that specialists cannot feel the soft tissues through the fingertips, which is critical in surveying the wellbeing status of the tissue. Giving firmness affectability to specialists amid these surgeries gives the capacity to portray and palpate soft tissues, and enables specialists to separate amongst ordinary and contaminated tissues. Likewise, such material criticism enables specialists to apply sufficient compel on the controlled delicate tissue; Consequently, keeping away from soft tissue harm amid surgery. Keeping in mind the end goal to recognize delicate tissue firmness, a few ideas of estimation have been presented. A standout amongst the most well-known systems relies upon the utilization of a compel on the soft tissue and the estimation of the related disfigurement/diversion [2]. Appropriately, the stiffness of the tissue can be computed.

ISSN: 2233-7857 IJFGCN

LITERATURE REVIEW

Hasegawa et al. [3] built up a multifunctional material sensor driven by an attractive field, which could quantify contact compel and in addition other physical amounts.

Muhammad et al. [4] designed and implemented a micro tactile sensor consisting of a thin silicone electrode diaphragm, cavity and silicone bottom. The diaphragm deflection, due to the applied pressure, is detected by measuring the change in capacitance between the diaphragm and the substrate. This concept of stiffness measurement has some limitations. In order to distinguish between the stiffness of the different tissues, a constant drive force must be applied. Therefore, it usually requires external equipment to supply a constant force, which makes the sensor more expensive [5]. Another concept of measurement was presented by Ju et al. [6], which is based on resonant frequency. They used a piezoelectric coated cantilever, which has a specific resonance frequency, and the change in resonance frequency that occurs when the sensor comes into contact with the tissue is used to detect tissue stiffness.

Murayama et al. [7] built up a piezoelectric resonator, with which they could separate between various examples of silicone elastic with various modules of Young. The above estimat io n thought encounters the reliance of its execution on the contact pressure between the sensor and the sensitive tissue. In this way, a consistent pressure is required to perceive different tissues. Engel et al. [8] built a material polymer sensor that can recognize the hardness of sensitive tissues. Hypothetically, the sensor yield was diagnostically figured on the premise of response drives in two springs, with various stiffness, in a two-spring design sensor. In any case, it was discovered tentatively that the expansion in connected pressure prompts an increment in the hardness of the deliberate tissue, for a similar tissue. Dargahi et al. [9] utilized a similar idea to create piezoelectric sensors equipped for measuring the aggregate constrain connected to the recognized question and also its consistence. Sensors by and large comprise of unbending and consistent components. The assurance of the congruity of the identified articles depends on the proportion of the constrain experienced by the unbending component to the aggregate compel connected to the sensor.

In light of a comparable thought of "applying two springs with fundamentally unique stiffness to soft tissues for soft tissue recognition," Fath El-Bab et al. [10] developed a definite arrangement technique, considering the stiffness tissue estimation go, to propel the shape parameters of the sensor to give high affectability and linearity of the sensor execution to procure the self-ruling execution of the Push detachment between the sensor and tissue utiliz ing ANSYS TOOL. The arrangement acknowledged a by and large level surface regarding the contact mesa. The different segment between the two mesas is been sufficiently far, with the goal that the disfigurements in each table impact the immaterial one.

In perspective of a comparative thought of pushing the sensor having two serpentine springs which is free of the different pushed between the sensor and the tissue, the whiteness of the soft tissue can be perceived utilizing the COMSOL TOOL which can be found rather than the execution of the ANSYS TOOL. The separation between two serpentine springs is taken as

ISSN: 2233-7857 IJFGCN

2mm by which increases the spatial resolution of the sensor, thus better performance can be obtained. Better performance of the sensor is obtained when compared with ANSYS TOOL.

DESIGN AND WORKING PRINCIPLE

The sensor is appeared as two springs, as appeared in Fig. 1, to be particular, Sl (low stiffness spring) and Sh (high stiffness spring).

The low and high stiffness springs have stiffness constants of kl and kh independently. The soft tissue has a steady stiffness ko. At the point where the two springs come into contact with the soft tissue, two distinct forces happen on the sides of the springs of high and low stiffness of the evaluations FH and FL, independently. By measuring FH and FL, stiffness of the soft tissues can be imparted as a Q component, as it shows up in the backup:

$$K_0 = \frac{K_h \; K_1 \; (1 - Q)}{(QK_1 - K_h)}$$

Where Q (= FH/FL) is a dimensionless variable. The yield of the sensor is called Q as the stiffness of the tissue, and ko can be assessed from Q utilizing (1).

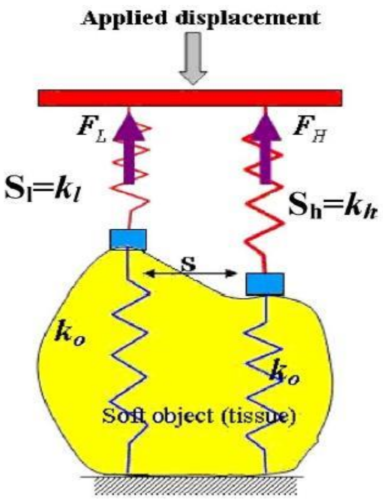

Fig 1 sensor model

SENSOR STRUCTURE AND DESIGN

The basic plan of the sensor took after the accompanying contemplations:

The association between the applied pressure and the relating deflection must be direct.

The measurements of the sensor components must be identified with the unbending nature picked.

The sensor structure is picked as a blend of silicon tones with different estimations (sensor segments). The cantilevered structure is picked due to its notoriety for linear behaviour of the force and displacement [11]. Then again, the cantilevered structure can be utilized as a spring with a touch of space permitting high spatial determination [12]. The cantilevered structure was utilized as a major aspect of a substantial number of MEMS exams [13-15]

The stiffness estimation of kh and kl can be accessed from the accompanying condition,

$$k = \frac{Ebt^3}{4l^3}$$

ISSN: 2233-7857 IJFGCN

In the light of 170 GPa Young's silicon (E) module, tolerating that the width (b) and thickness (t) of a l bulges are 300 µm and 50 µm independently. Accordingly, it was watched that the lengths (l) of the low and high stiffness bulges were 2100 µm and 655 µm, separately.

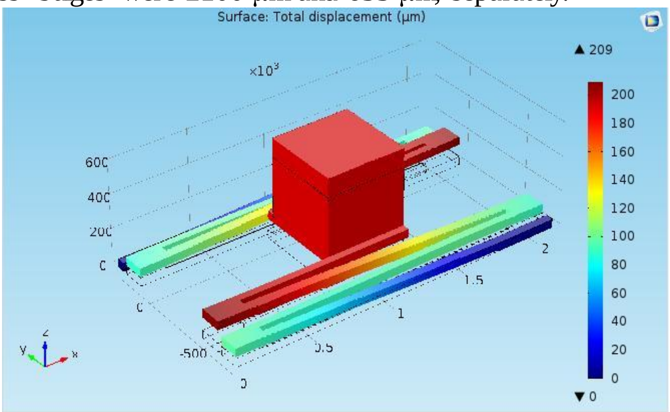

Fig 2 Low stiffness spring.

Table 1: Force vs displacement of low stiffness spring.

Force (mN)	Displacement(um)
10	104
20	209
40	418
60	627
80	836

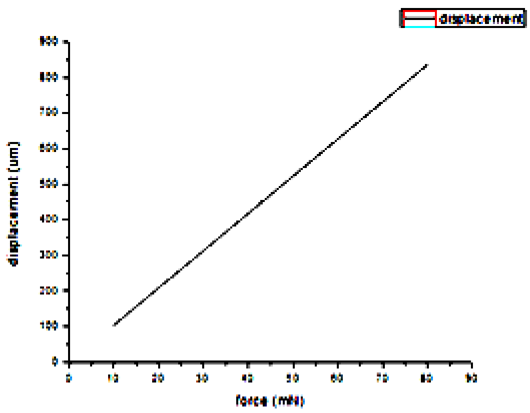

ISSN: 2233-7857 IJFGCN

.International Journal of Future Generation Communication and Networking
Vol. 13, No. 3, (2020), pp. 2979–2989

Fig 3 A linear Force – displacement for low stiffness spring.

For various applied forces observe the displacement changes for both the low stiffness and high stiffness springs. Fig 2 low stiffness constant spring with force as input, displacement.

as output. Table 1 shows the force vs displacement values and F ig 3 shows a linear graph between force and displacement for a low stiffness constant spring. A linear relationship is obtained by the selected dimensions for the low stiffness spring. Fig 4 shows high stiffness constant spring. Apply force to the high stiffness spring and obtain the displacement values. Thus the selected dimensions gives the linear relationship for low stiffness and high stiffness springs as previously discussed.

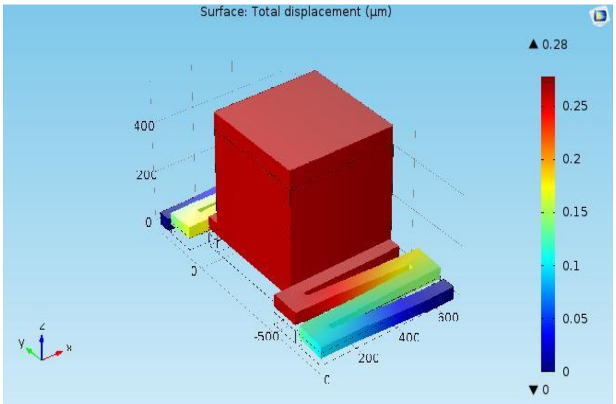

Fig 4 High stiffness spring

Table 2 :Force vs displacement of high stiffness spring.

Force (mN)	Displacement(um)
1	0.28
2	0.56
3	0.83
4	1.11
5	1.39

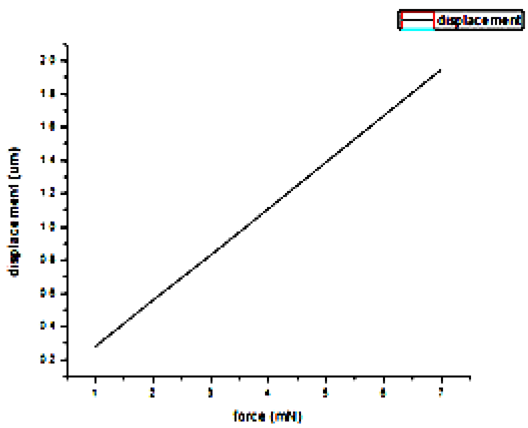

ISSN: 2233-7857 IJFGCN

Fig 5 A linear Force – displacement for high stiffness spring.

Figure 3 demonstrates that the chose estimation of s1 gave a direct Force move association with kl = 172 N/m, which is near the desired gauge of 170 N/m. A similar investigation is finished with Sh. Table 2 shows the force vs displacement values and Figure 5 demonstrates that the selected measurement of Sh gave a direct compel relocation association with kl = 5669 N/m, which is near the coveted estimation of 5700 N/m.

Now observe the relation between Force applied and stress because the sensor is based on the concept of piezo-resistor at the maximum stress location. Force is applied to the low stiffness spring and stress is observed. Different force values are applied and stress values are noted.

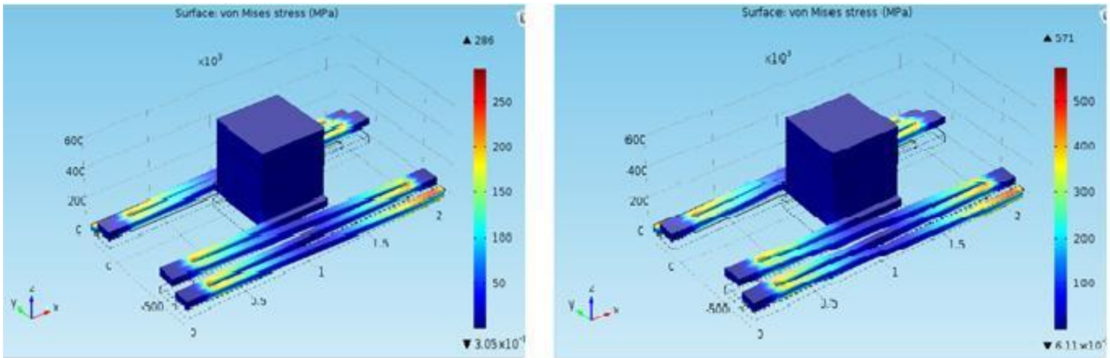

Fig 6 stress induced in low stiffness

Fig 6 shows the stress induced in the low stiffness spring, Force is applied to the low stiffness spring and stress is observed.

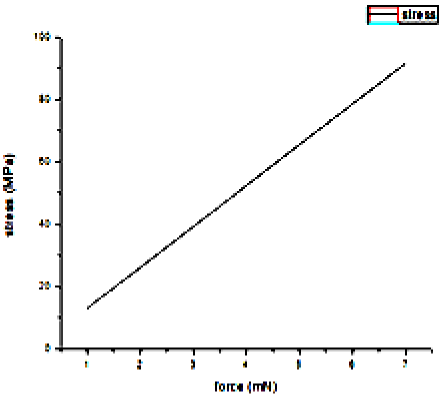

Fig 7 Linear relation between stress and force of a low stiffness spring.

Similarly force is applied and stress is observed for the high stiffness spring also. Fig 8 shows stress induced in the high stiffness spring. Fig 7 and Fig9 shows a linear relation is obtained when force versus stress is plotted for both low and high stiffness springs.

ISSN: 2233-7857 IJFGCN

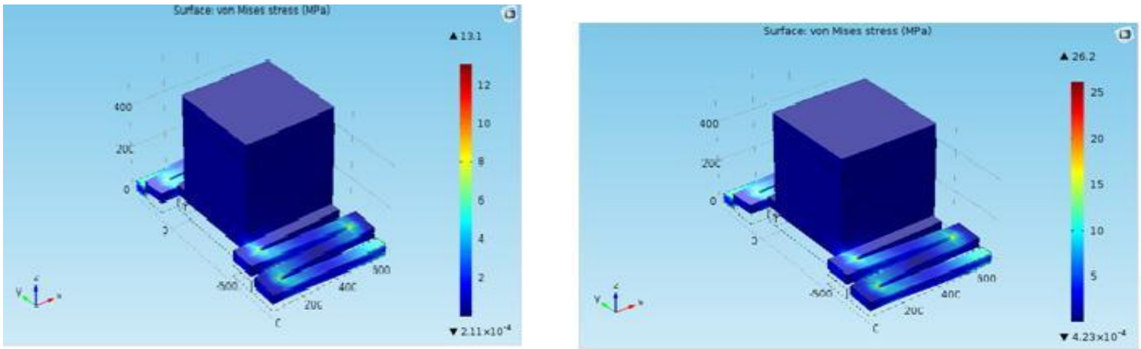

Fig 8 stress induced in high stiffness spring.

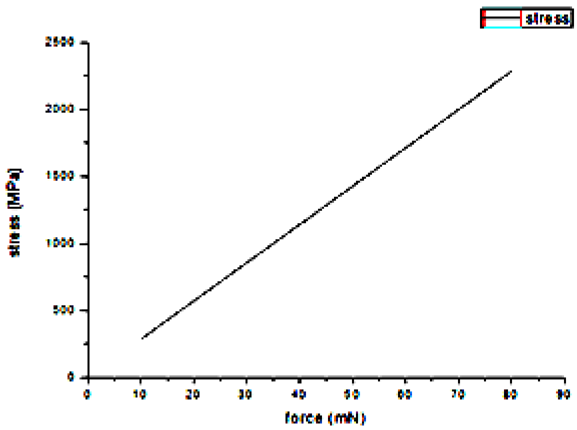

Fig 9 A Linear relation between stress and force for high stiffness spring.

FEM Analysis

The sensor structure is designed using low stiffness and high stiffness springs using the COMSOL software. The sensor is spoken to by two serpentine springs. The soft tissue is thought to be homogeneous and poisons ratio of 0.49 and measurements of 10 mm * 10 mm * 10 mm and Young's modulus of 0.25, 0.5, 0.75 and 1 MPa . The Young's modulus of 0.25, 0.5, 0.75 and 1 Mpa speaks to the tissue solidness ko of 166, 333, 500 and 833 N/m. The sensor is appeared with two serpentine springs of thickness 50um. Fig. 10 demonstrates the FE model of the sensor with two serpentine springs with applied force and output as stress. These observations shows that when sensor is made to contact with soft tissue there exist a force opposite to the sensor which consist of two serpentine springs with two different spring constants and that force can be calculated using piezo resistors. Thus the soft tissue can be detected whether it is healthy or diseased. Here the inflexibility of the soft tissues is autonomous of the applied force. The sensor perusing is the stress ratio (Q) on the spring mesa of high and low stiffness. Figure 11 demonstrates the diagram between the distinctive estimations of the young's modulus and the sensor yield (Q), which is the proportion of strengths in high and low firmness springs. Fig. 12 demonstrates the recreation of the sensor yield, applying different force values and acquiring the yield of the sensor for various estimations of Young's modulus. By perception unmistakably the yield of the sensor is free of the applied force which is fundamental.

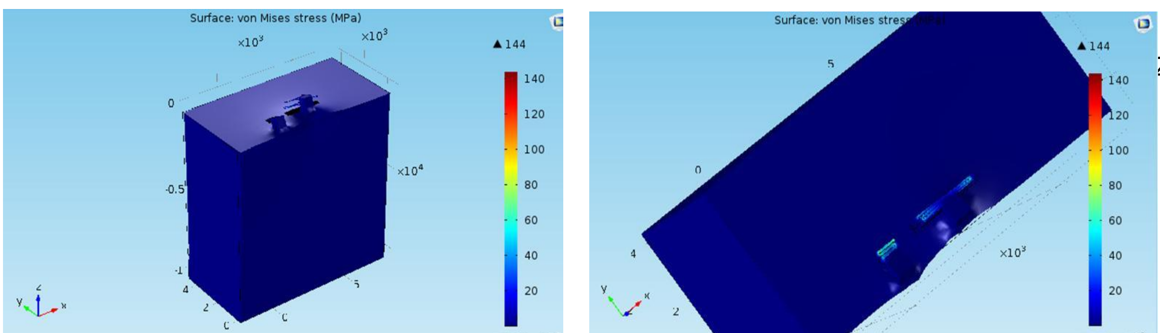

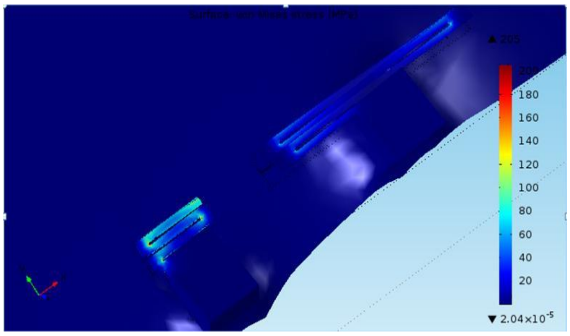

Fig 10 Finite element model of a sensor

Comparison table

Table 3 shows the comparison of the theoretical and practical values. This shows that the sensor output which is obtained from the simulation values of the sensor with the COMSOL TOOL is very similar to that of the theoretical values.

Table 4 shows the Comparison table for the present sensor output values which are simulated using COMSOL TOOL with the Ahmed M. R. Fath El Bab's sensor output which is simulated using ANSYS TOOL. This table shows that the sensor output values are improved when compared with the previous results which are simulated using ANSYS TOOL.

Table 3:comparision of theoretical and practical sensor output values

parameter	Sensor output(Q)	Sensor output(Q)
Young's modulus	Theoretical values	Practical values
0.25	1.92	1.86
0.5	2.7	2.68
0.75	3.62	3.5
1.0	4.4	4.3
1.25	5.2	5.1

ISSN: 2233-7857 IJFGCN

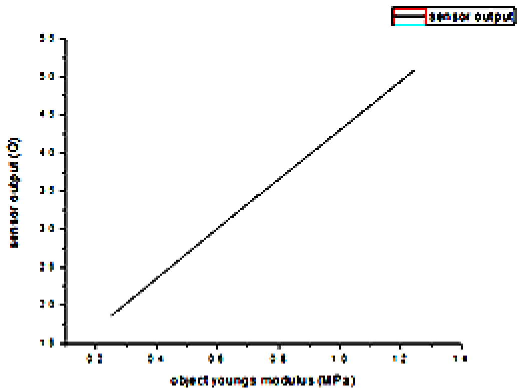

Fig 11 Simulation of the sensor output.

Table: 4 Comparison of sensor output of previous and present simulation

APPLIED FORCE	parameter	Sensor output-stress (Q)	Sensor output-stress(Q)
Milli-Newtons	Young's modulus(MPa)	Ahmed M. R. Fath El Bab's simulation	Present simulation
10-80	0.25	1.8	1.86
10-80	0.5	2.5	2.68
10-80	0.75	3.3	3.5
10-80	1	4.1	4.3
10-80	1.25	4.8	5.1

From this table it is clear that we got more sensitivity compared to the others in terms of displacement and stress.

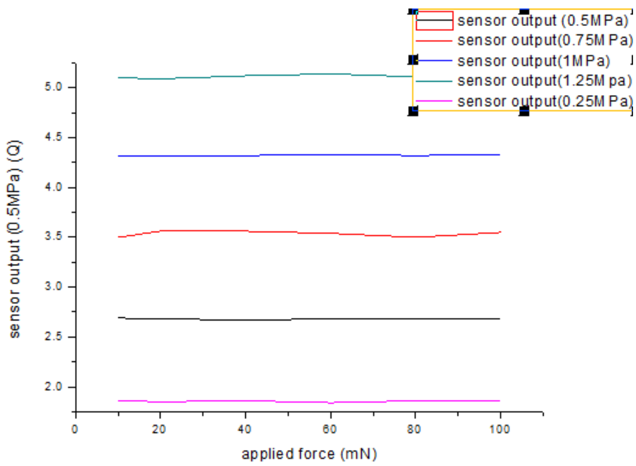

ISSN: 2233-7857 IJFGCN

Fig 12 Simulation of the sensor output.

Conclusi on

The micromachined tactile sensor is designed and simulated using the COMSOL TOOL and compared with the previous simulations using ANSYS TOOL. The micromachined tactile sensor is designed with two serpentine springs with different spring constants namely 172 and 5669 N/m. In Mohamed E. H. Eltaib paper the separation between the two serpentine springs is 3mm, but in the present paper the separation between two serpentine springs is 2mm thus the spatial resolution is increased. For the tissues having young's modulus of 0.25, 0.5MPa the sensor output (Q) is almost similar in both previous and present cases but for the tissue with young's modulus of 0.75, 1, 1.25MPa. It enhances the yield execution of the present sensor, which is reproduced utilizing COMSOL TOOL contrasted with the yield of the sensor that is mimicked with ANSYS TOOL. Subsequently, the execution of the sensor increments and gets practically precise esteems with the hypothetical esteems.

Acknowledgment

The authors would like to thank NPMASS scheme for establishing national MEMS Design Centres in AP which is supported by IISc, Bangalore for providing the necessary design facilities

References

1. M. I. Tiwana, S. J. Redmond, and N. H. Lovell, "A review of tactile sensing technologies with applications in biomedical engineering," Sens. Actuators Phys., vol. 179, pp. 17–31,2012.
2. Y. B. Fu, C. K. Chui, and C. L. Teo, "Liver tissue characterization from uniaxial stres s–strain data using probabilistic and inverse finite element methods," J. Mech. Behav. Biomed. Mater., vol. 20, pp. 105–112, 2013. [3] Y. Hasegawa, H. Sasaki, T. Ando, M. Shikida, K. Sato, and K. Itoigawa, "Multifunctional active tactile sensor using magnetic micro actuator," in Micro Electro Mechanical Systems, 2005. MEMS 2005. 18th IEEE International Conference on, 2005, pp. 275–278.
3. [4] H. B. Muhammad, C. M. Oddo, L. Beccai, M. J. Adams, M. C. Carrozza, D. W. Hukins, and M. C. Ward, "Development of a biomimetic MEMS based capacitive tactile sensor," Procedia Chem., vol. 1, no. 1, pp. 124–127, 2009.
4. G.R.K Prasad et.al "Comparative Analysis Of Mems Capacitive Pressure Sensor For Detection Of Tremors In Parkinson's Disease" ,JATIT, Vol:95, Issue:9,pp:2023-2030,May 2017.
5. N.Siddaiah et.al "Design and analysis of piezo electric energy harvester used in car tyres" IJCTA, 9(34),
6. pp:349-359,2016.
7. [7] Y. Murayama and S. Omata, "Fabrication of micro tactile sensor for the meas urement of micro-scale local elasticity," Sens. Actuators Phys., vol. 109, no. 3, pp. 202–207, 2004.
8. [8] J. Engel, J. Chen, Z. Fan, and C. Liu, "Polymer micromachined multimodal tactile s ensors," Sens. Actuators

ISSN: 2233-7857 IJFGCN

9. Phys., vol. 117, no. 1, pp. 50–61, 2005.
10. [9] S. Sokhanvar, M. Packirisamy, and J. Dargahi, "A multifunctional PVDF based tactile sensor for minimally invasive surgery," Smart Mater Struct.vol. 16, no. 4, pp. 989–998, Aug. 2007.
11. [10] A. M. R. Fath El Bab, T. Tamura, K. Sugano, T. Tsuchiya, O. Tabata, M. E. H. Eltaib, and M. M. Sallam, "Design and simulation of a tactile sensor for soft-tissue compliance detection," IEEJ Trans. Sens. Micromach., vol. 128-E, no. 5, pp. 186–192, 2008.
12. [11] R. Ellis, S. Ganeshan, and S. Lederman, "A tactile sensor based on thin-plate deformation," Robotica, vol.
12, no. 04, pp. 343–351, 1994.
13. [12]B. Charlot, F. Parrain, N. Galy, S. Basrour, and B. Courtois, "A sweeping mode integrated fingerprint sensor with 256 tactile microbeams," Micro electro mechanical Systems, Journal of, vol. 13, no. 4, pp. 636–644, 2004. [13] "Tunable {MEMS} cantilever resonators electro thermally actuated and piezoelectrically sensed," Microelectronic Engineering, vol. 145, no. 0, pp. 38 – 42, 2015, micro/Nano Devices & Systems 2014.
14. [14]N. Kilinc, O. Cakmak, A. Kosemen, E. Ermek, S. Ozturk, Y. Yerli, Z. Z. Ozturk, and H. Urey, "Fabrication
of 1d zno nanostructures on {MEMS} cantilever for {VOC} sensor application," Sensors and Actuators B: Chemical, vol. 202, no. 0, pp. 357 – 364, 2014.
15. [15] M. Mihara, A. Nozawa, T. Abe, M. Okuyama, H. Noma, T. Azuma, and M. Sohgawa, "Tactile sensor using
micro-cantilever with bifeo3piezoelectric film," IEEJ Transactions on Sensors and Micromachines, vol. 135, no.
5, pp. 158–164, 2015.

ISSN: 2233-7857 IJFGCN